Cosmic Ray Anisotropy

Markus Ahlers

Niels Bohr Institute, Copenhagen

Virtual Workshop on
"Multimessenger high energy astrophysics in the era of LHAASO"
July 27–29, 2020

The Niels Bohr International Academy

VILLUM FONDEN

UNIVERSITY OF COPENHAGEN

Galactic Cosmic Rays

- *Standard paradigm:* Galactic CRs accelerated in **supernova remnants**

✔ sufficient power: $\sim 10^{-3} \times M_\odot$ with a rate of ~ 3 SNe per century [Baade & Zwicky'34]

- galactic CRs via diffusive shock acceleration?

$$n_{\rm CR} \propto E^{-\gamma} \qquad \text{(at source)}$$

- energy-dependent **diffusion** through Galaxy

$$n_{\rm CR} \propto E^{-\gamma-\delta} \qquad \text{(observed)}$$

- arrival direction **mostly isotropic**

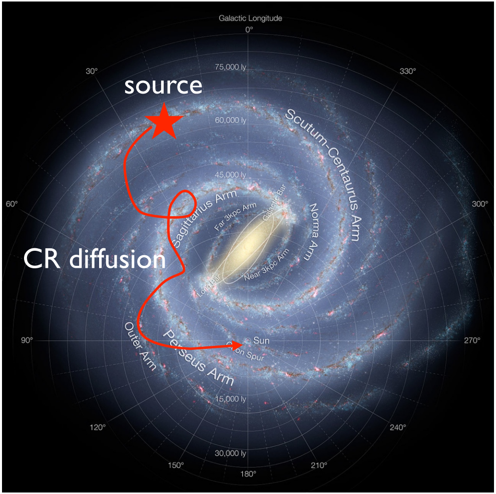

Galactic Cosmic Ray Anisotropy

Cosmic ray anisotropies up to the level of **one-per-mille** at various energies
(Super-Kamiokande; Milagro; ARGO-YBJ; EAS-TOP, Tibet AS-γ; IceCube; HAWC)

Anisotropy = Relative Intensity - 1

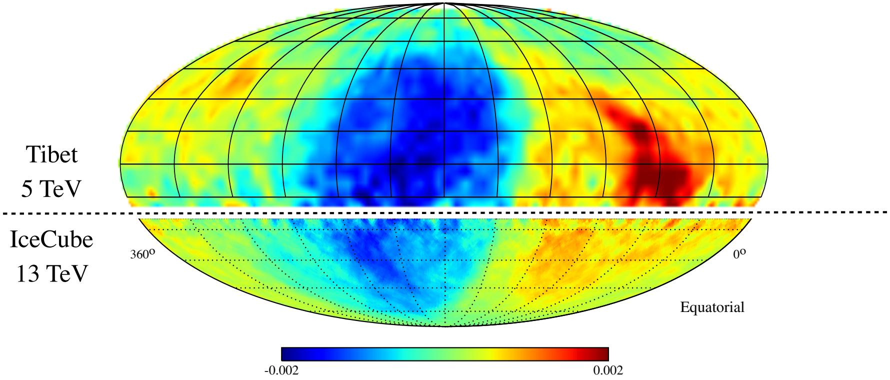

[*e.g.* review by MA & Mertsch'16]

Galactic Cosmic Ray Anisotropy

Cosmic ray anisotropies up to the level of **one-per-mille** at various energies
(Super-Kamiokande; Milagro; ARGO-YBJ; EAS-TOP, Tibet AS-γ; IceCube; HAWC)

Energy-Dependence

Large-scale (dipole) anisotropy has strong energy dependence
with phase-flip around 100 TeV.

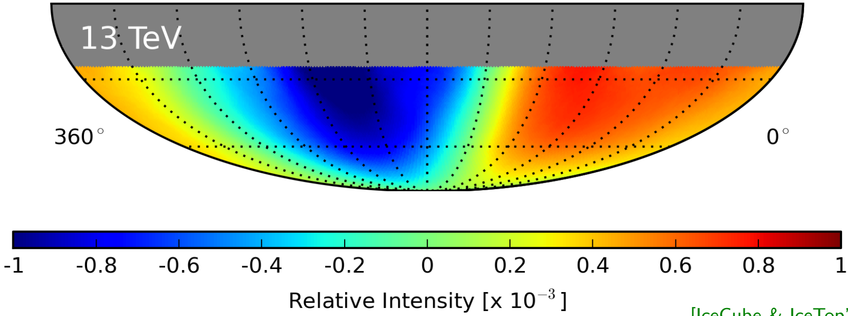

[IceCube & IceTop'16]

Energy-Dependence

Large-scale (dipole) anisotropy has strong energy dependence
with phase-flip around 100 TeV.

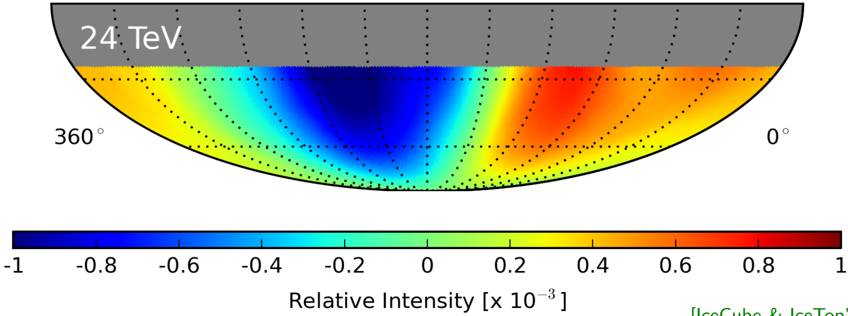

[IceCube & IceTop'16]

Energy-Dependence

Large-scale (dipole) anisotropy has strong energy dependence with phase-flip around 100 TeV.

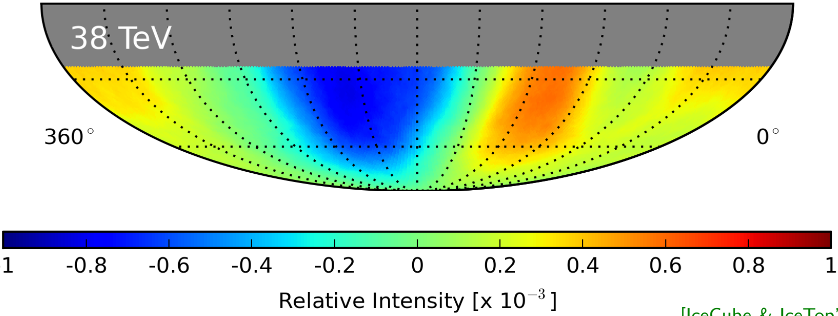

[IceCube & IceTop'16]

Energy-Dependence

Large-scale (dipole) anisotropy has strong energy dependence
with phase-flip around 100 TeV.

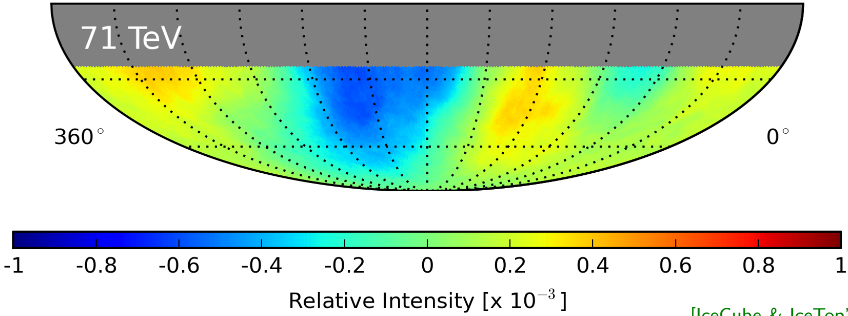

[IceCube & IceTop'16]

Energy-Dependence

Large-scale (dipole) anisotropy has strong energy dependence
with phase-flip around 100 TeV.

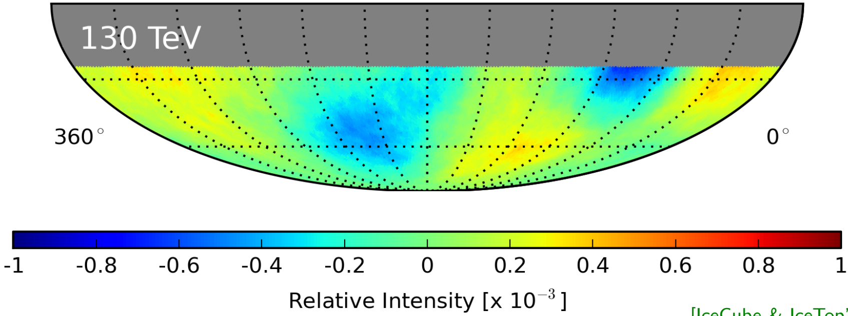

[IceCube & IceTop'16]

Energy-Dependence

Large-scale (dipole) anisotropy has strong energy dependence with phase-flip around 100 TeV.

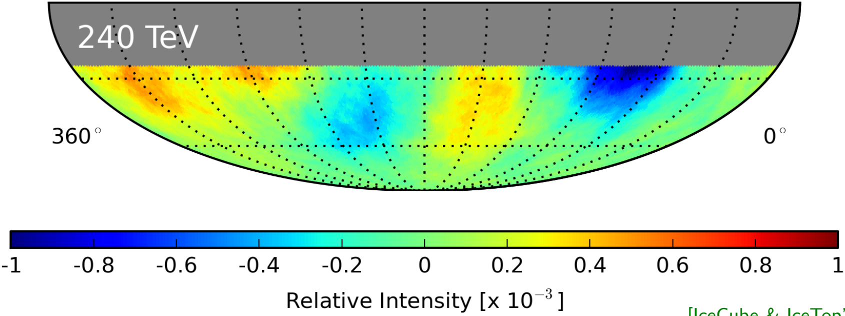

[IceCube & IceTop'16]

Energy-Dependence

Large-scale (dipole) anisotropy has strong energy dependence
with phase-flip around 100 TeV.

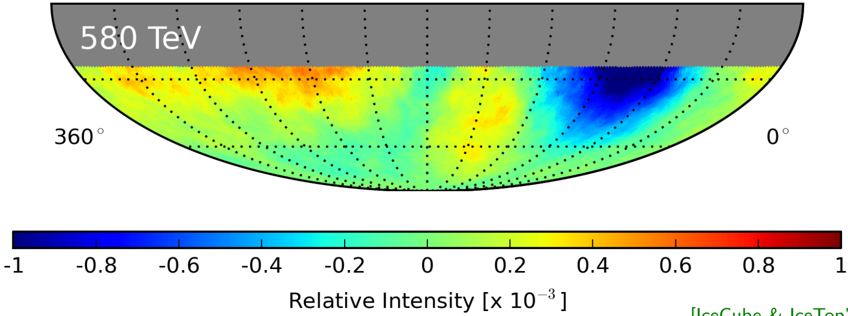

[IceCube & IceTop'16]

Energy-Dependence

Large-scale (dipole) anisotropy has strong energy dependence
with phase-flip around 100 TeV.

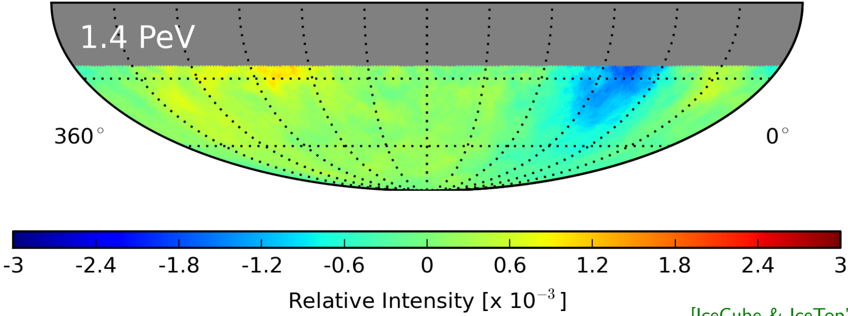

[IceCube & IceTop'16]

Energy-Dependence

Large-scale (dipole) anisotropy has strong energy dependence
with phase-flip around 100 TeV.

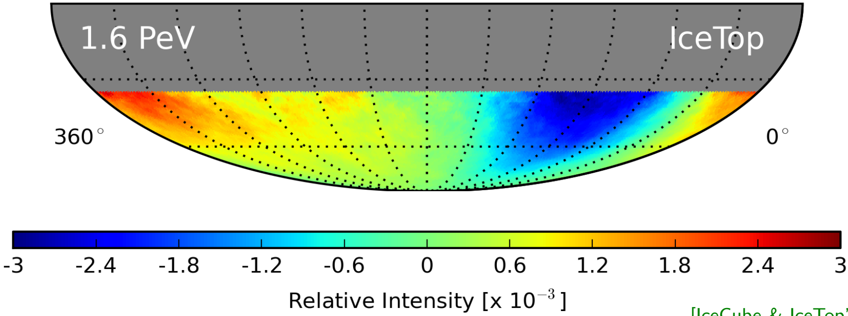

[IceCube & IceTop'16]

Energy-Dependence

Large-scale (dipole) anisotropy has strong energy dependence
with phase-flip around 100 TeV.

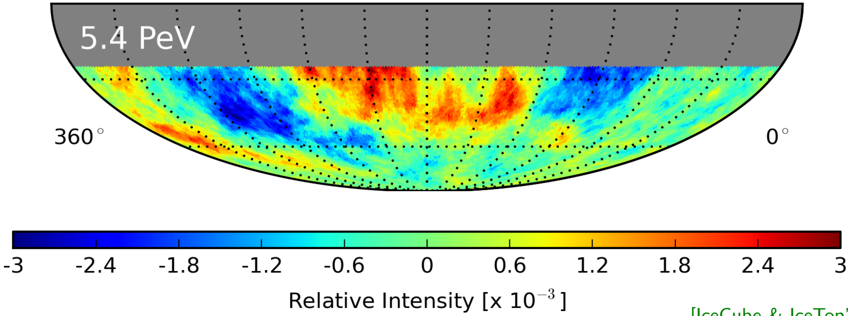

[IceCube & IceTop'16]

Time-Dependence

No significant variation of TeV-PeV anisotropy over time scales of $\mathcal{O}(10)$ years.

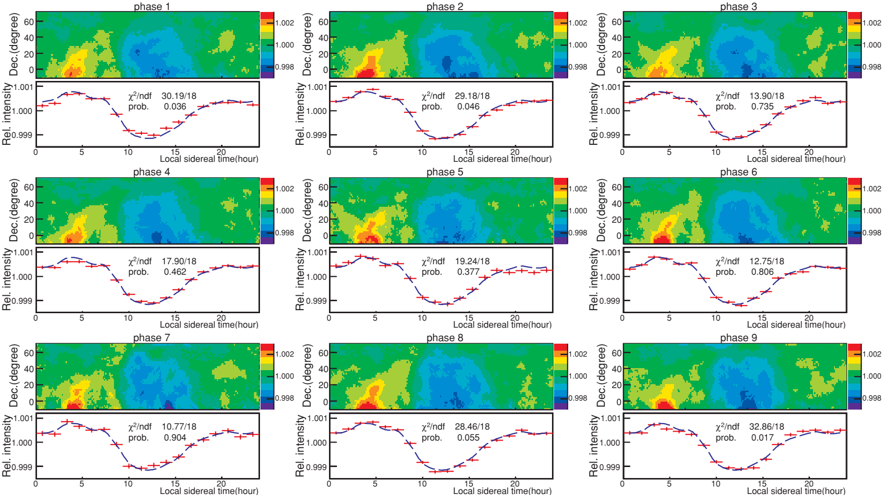

[Tibet-ASγ'10]

Recent Highlight: Auger Dipole Anisotropy

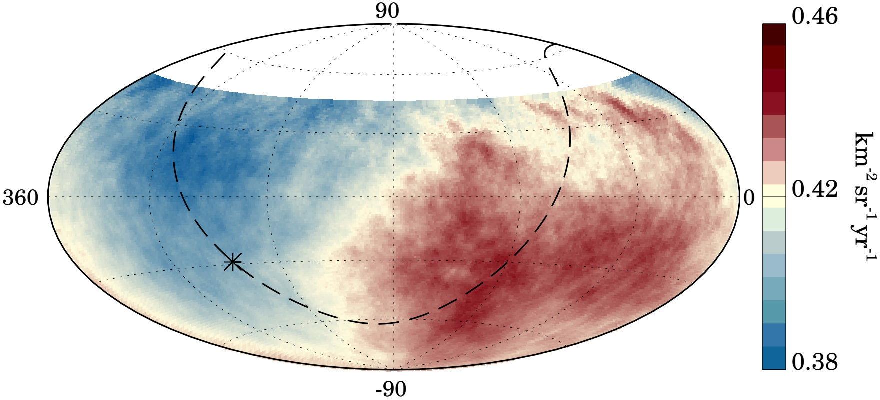

Energy [EeV]	Dipole component d_z	Dipole component $d_\perp$	Dipole amplitude d	Dipole declination δ_d [°]	Dipole right ascension α_d [°]
4 to 8	-0.024 ± 0.009	$0.006^{+0.007}_{-0.003}$	$0.025^{+0.010}_{-0.007}$	-75^{+17}_{-8}	80 ± 60
8	-0.026 ± 0.015	$0.060^{+0.011}_{-0.010}$	$0.065^{+0.013}_{-0.009}$	-24^{+12}_{-13}	100 ± 10

[Auger, Science'17]

Anisotropy Reconstruction

Reconstruction Methods

✘ data is strongly **time-dependent**:

- detector deployment/maintenance
- atmospheric conditions (day/night, seasons)
- power outages,...

✘ **local anisotropies** of detector:

- detector geometry
- mountains
- geo-magnetic fields,...

- two analysis strategies:
  - **Monte-Carlo & monitoring** (limited by **systematic** uncertainties)
  - **data-driven likelihood methods** (limited by **statistical** uncertainties)

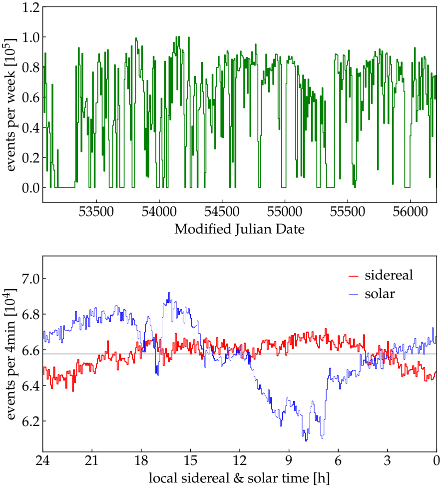

example: KASCADE-Grande data

[MA'19]

Data-Driven: East-West Method

- Strong time variation of cosmic ray background level can be compensated by differential methods. [*e.g.* Bonino *et al.*'11]
- **East-West asymmetry:**

$$A_{\rm EW}(t) \equiv \frac{N_{\rm E}(t) - N_{\rm W}(t)}{N_{\rm E}(t) + N_{\rm W}(t)} \simeq \underbrace{\Delta\alpha \frac{\partial}{\partial\alpha}\delta I(\alpha,0)}_{\textbf{if dipole!}} + \underbrace{\text{const}}_{\text{local asym.}}$$

- For instance, binned KASCADE-Grande data (2.7 PeV, 6.1 PeV & 33 PeV): [MA'19]

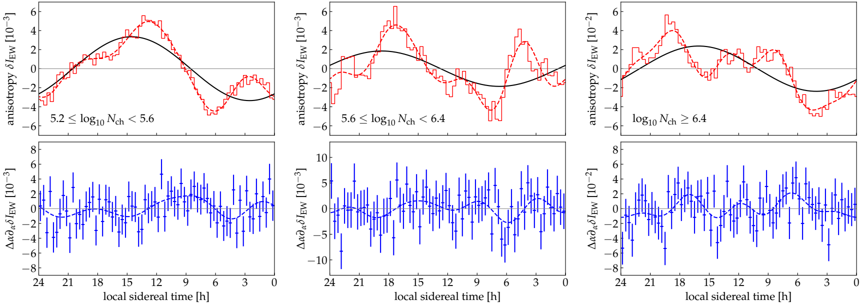

(no significant dipole anisotropy found)

Data-Driven: Likelihood Reconstructions

✘ East-West method introduces cross-talk between higher multipoles, regardless of field of view.

➜ Alternatively, data can be analyzed to *simultaneously* reconstruct:

- **relative acceptance** $\mathcal{A}(\varphi,\theta)$ (in local coordinates)
- **relative intensity** $I(\alpha,\delta)$ (in equatorial coordinates)
- **background rate** $\mathcal{N}(t)$ (in sidereal time)

- expected number of CRs observed in sidereal time bin τ and local coordinate i:

$$\mu_{\tau i} = \mu(\mathcal{I}_{\tau i}, \mathcal{N}_\tau, \mathcal{A}_i)$$

- reconstruction via maximum likelihood:

$$\mathcal{L}(n|I,\mathcal{N},\mathcal{A}) = \prod_{\tau i} \frac{(\mu_{\tau i})^{n_{\tau i}} e^{-\mu_{\tau i}}}{n_{\tau i}!}$$

- Maximum can be reconstructed by iterative methods. [MA *et al.*'15]

➜ used in joint IceCube & HAWC analysis [IceCube & HAWC'18]

Example: KASCADE-Grande

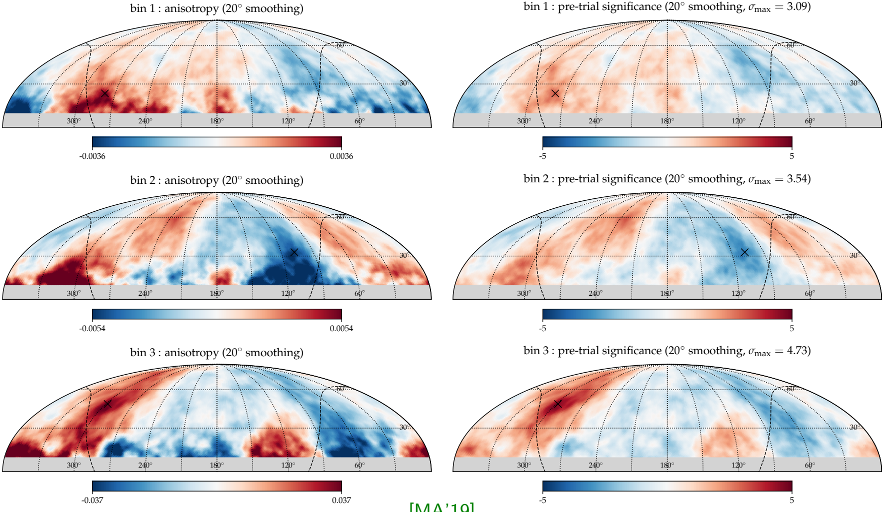

[MA'19]

Sidereal anisotropy in the KASCADE-Grande data with median energy of 2.7 PeV (bin 1), 6.1 PeV (bin 2) and 33 PeV (bin 3).

Small-Scale Feature At the 2nd Knee?

bin 3 : post-trial significance (20° smoothing, $\sigma_{\max} = 4.16$)

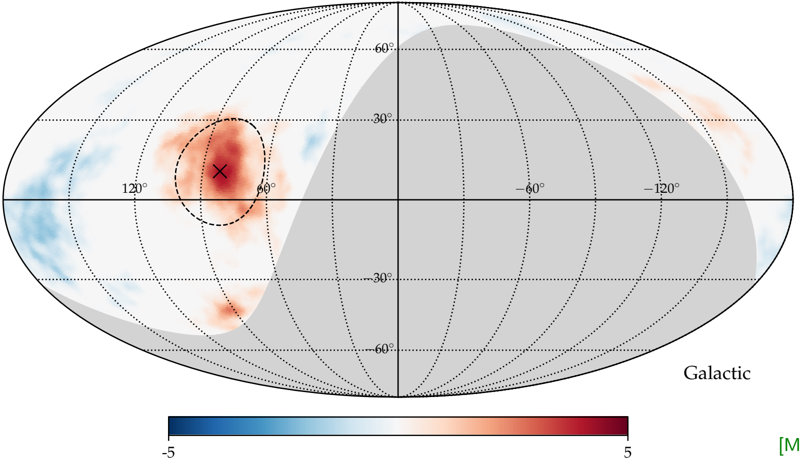

[MA'19]

Small-scale anisotropy of 33 PeV cosmic rays overlaps with Cygnus region.
(gyro radius < 10 pc; neutron decay length $\simeq 300$ pc)

Issues with Data-Driven Reconstruction

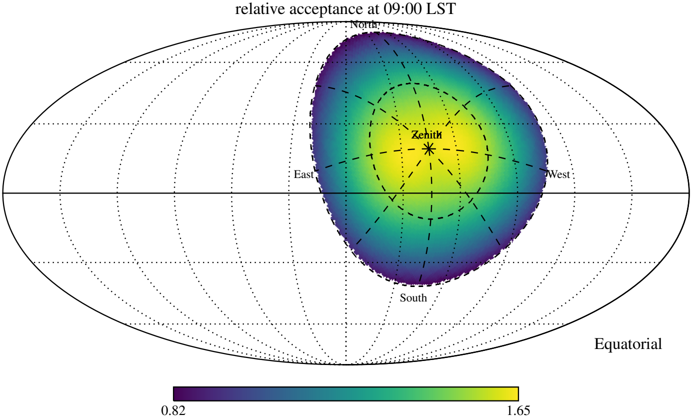

- ground-based detectors need to be **calibrated** by CR data
- true CR dipole defined by amplitude A_1, and orientation (RA,DEC) $= (\alpha_1,\delta_1)$

✘ observable: **projected dipole** with amplitude $A_1' = A_1 \cos\delta_1$ and orientation $(\alpha_1,0)$

[Iuppa & Di Sciascio'13; MA *et al.*'15]

Issues with Data-Driven Reconstruction

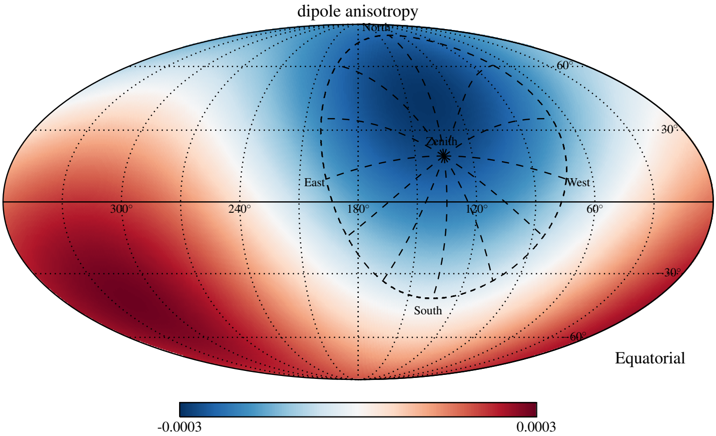

- ground-based detectors need to be **calibrated** by CR data
- true CR dipole defined by amplitude A_1, and orientation (RA,DEC) $= (\alpha_1,\delta_1)$

✘ observable: **projected dipole** with amplitude $A_1' = A_1 \cos\delta_1$ and orientation $(\alpha_1,0)$

[Iuppa & Di Sciascio'13; MA *et al.*'15]

Issues with Data-Driven Reconstruction

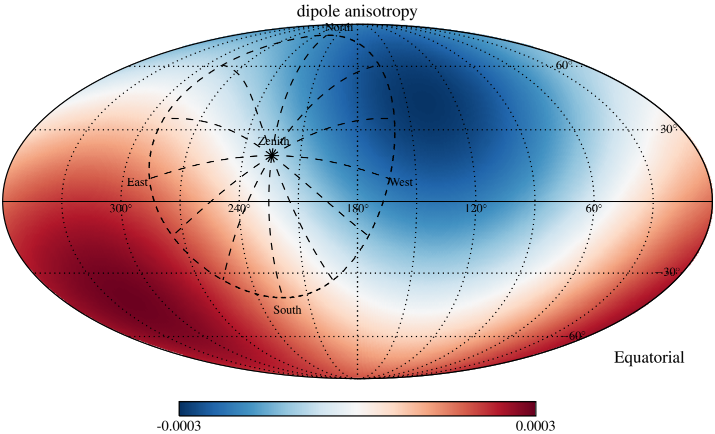

- ground-based detectors need to be **calibrated** by CR data
- true CR dipole defined by amplitude A_1, and orientation (RA,DEC) $= (\alpha_1, \delta_1)$

✗ observable: **projected dipole** with amplitude $A_1' = A_1 \cos\delta_1$ and orientation $(\alpha_1, 0)$

[Iuppa & Di Sciascio'13; MA *et al.*'15]

Issues with Data-Driven Reconstruction

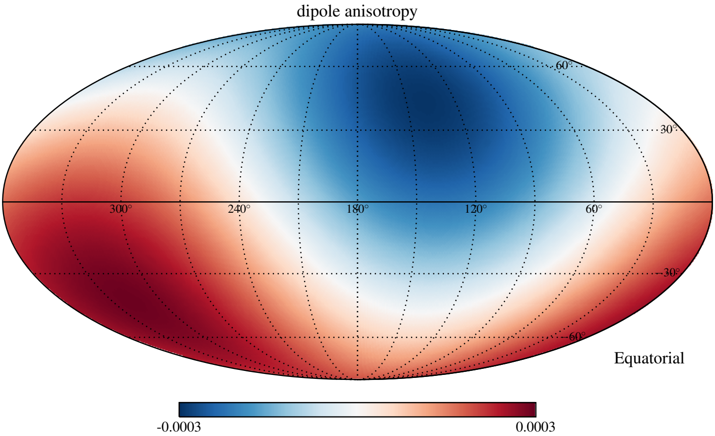

- ground-based detectors need to be **calibrated** by CR data
- true CR dipole defined by amplitude A_1, and orientation (RA,DEC) $= (\alpha_1,\delta_1)$

✘ observable: **projected dipole** with amplitude $A_1' = A_1 \cos\delta_1$ and orientation $(\alpha_1,0)$

[Iuppa & Di Sciascio'13; MA *et al.*'15]

Issues with Data-Driven Reconstruction

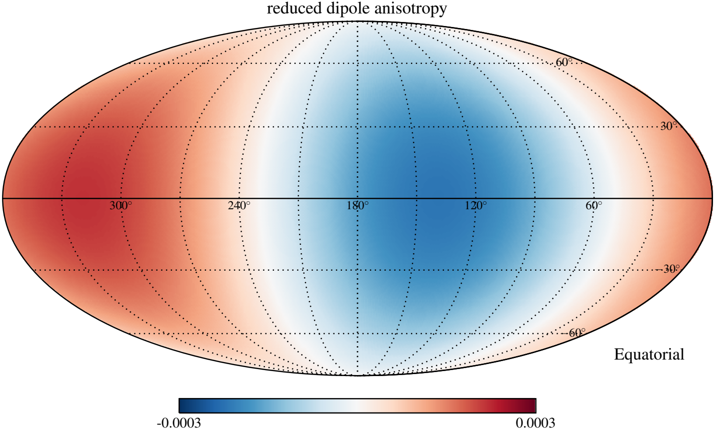

- ground-based detectors need to be **calibrated** by CR data
- true CR dipole defined by amplitude A_1, and orientation (RA,DEC) $= (\alpha_1,\delta_1)$

✘ observable: **projected dipole** with amplitude $A_1' = A_1 \cos\delta_1$ and orientation $(\alpha_1,0)$

[Iuppa & Di Sciascio'13; MA *et al.*'15]

Take-Away on Dipole Reconstruction

Data-driven methods of anisotropy reconstructions used by ground-based observatories are **only sensitive to equatorial dipole** (or, more generally, to all $m \neq 0$ multipoles)

$$\Delta\delta_\perp \sim \frac{1}{\sqrt{N_{\rm tot}}} \qquad \mathcal{N} \sim \frac{4\pi}{N_{\rm tot}}$$

Monte-Carlo-based methods of anisotropy reconstructions are sensitive to the full dipole, but are **limited by systematic uncertainties**.

Large-Scale Anisotropy

Cosmic Ray Dipole Anisotropy

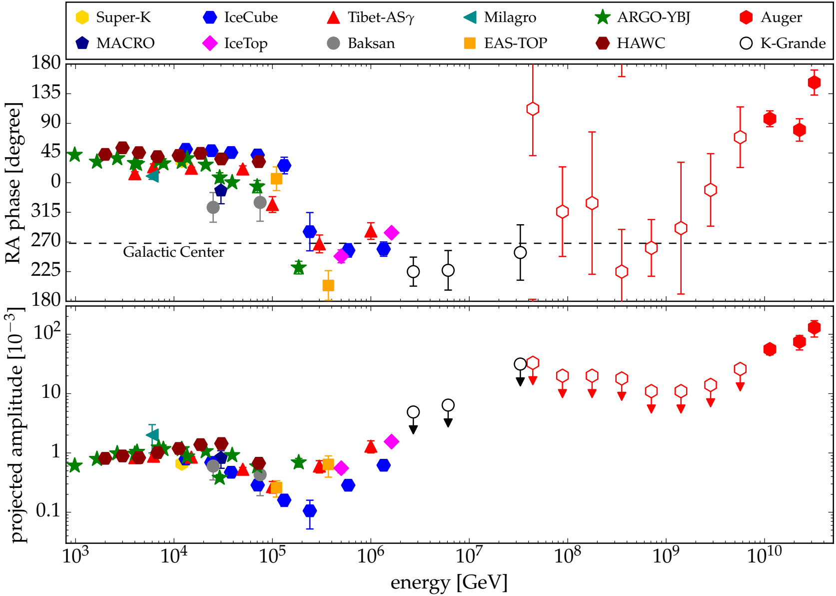

Cosmic Ray Dipole Anisotropy

- Spherical harmonics expansion of relative intensity yields:

$$I(\Omega) = 1 + \underbrace{\delta \cdot \widehat{\mathbf{n}}(\Omega)}_{\text{dipole}} + \sum_{\ell \geq 2} \sum_{m} a_{\ell m} Y^{\ell m}(\Omega)$$

- cosmic ray density $n_{\rm CR} \propto E^{-\Gamma_{\rm CR}}$ and dipole vector δ from **diffusion theory**:

$$\underbrace{\partial_t n_{\rm CR} \simeq \nabla(\mathbf{K}\nabla n_{\rm CR}) + Q_{\rm CR}}_{\text{diffusion equation}} \quad \text{and} \quad \underbrace{\delta \simeq 3\mathbf{K}\nabla n_{\rm CR}/n_{\rm CR}}_{\text{from Fick's law}}$$

- diffusion tensor $\mathbf{K}$ in general anisotropic (background field $\mathbf{B}$):

$$K_{ij} = \kappa_{\parallel}\widehat{B}_i\widehat{B}_j + \kappa_{\perp}(\delta_{ij} - \widehat{B}_i\widehat{B}_j) + \kappa_A \epsilon_{ijk}\widehat{B}_k$$

- **relative motion** v of the observer in plasma rest frame ($\star$): [Compton & Getting'35]

$$\delta = \delta^{\star} + \underbrace{(2 + \Gamma_{\rm CR})v/c}_{\text{Compton-Getting effect}}$$

TeV-PeV Dipole Anisotropy

- reconstructed diffuse dipole:

$$\delta^\star = \delta - \underbrace{(2+\Gamma_{\rm CR})\boldsymbol{\beta}}_{\text{Compton-Getting}} = 3\mathbf{K}\cdot\nabla n^\star/n^\star$$

- projection onto equatorial plane: →

$$\delta^\star_{\rm EP} = (\delta^\star_{\rm 0h}, \delta^\star_{\rm 6h})$$

- **strong regular magnetic fields** in the local environment

→ diffusion tensor reduces to **projector**:
[*e.g.* Mertsch & Funk'14; Schwadron *et al.*'14]

$$K_{ij} \to \kappa_\parallel \widehat{B}_i \widehat{B}_j$$

- TeV–PeV dipole data consistent with magnetic field direction inferred by IBEX data [McComas *et al.*'09]

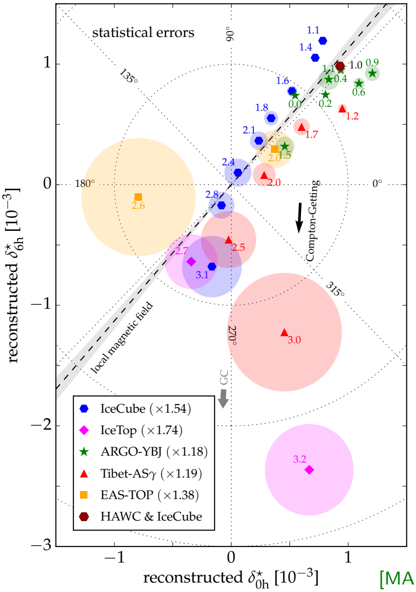

[MA'17]

Known Local Supernova Remnants

- projection maps source gradient onto $\widehat{\mathbf{B}}$ **or** $-\widehat{\mathbf{B}}$

➜ **dipole phase** α_1 depends on orientation of magnetic hemispheres

- intersection of magnetic equator with Galactic plane defines two source groups:

$$120^\circ \lesssim l \lesssim 300^\circ \to \alpha_1 \simeq 49^\circ$$

$$-60^\circ \lesssim l \lesssim 120^\circ \to \alpha_1 \simeq 229^\circ$$

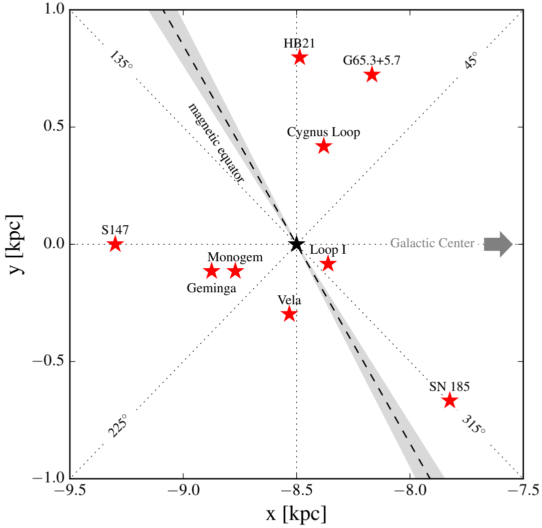

Phase-Flip by Vela SNR?

- 1–100 TeV phase indicates dominance of a local source within longitudes:

$$120^\circ \lesssim l \lesssim 300^\circ$$

- **plausible scenario: Vela SNR** [MA'16]
  - *age* : $\simeq 11,000$ yrs
  - *distance* : $\simeq 1,000$ lyrs
  - *SNR rate* : $\mathcal{R}_{\rm SNR} = 1/30\,{\rm yr}^{-1}$
  - *(effective) isotropic diffusion*:

$$K_{\rm iso} \simeq 4 \times 10^{28} (E/3{\rm GeV})^{1/3} {\rm cm}^2/{\rm s}$$

  - *Galactic half height* : $H \simeq 3$ kpc
  - *instantaneous CR emission* ($Q_\star$)

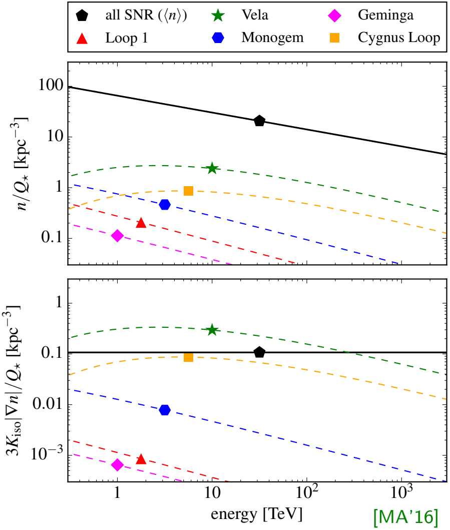

Position of SNR

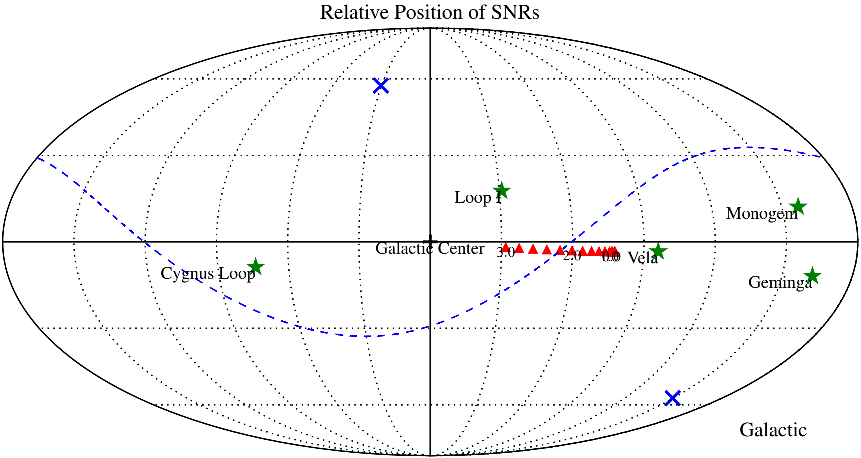

Relative position of the five closest known SNRs. The magnetic field direction (IBEX) is indicated by blue $\times$ and the **magnetic horizon** by a dashed line.

Position of SNR

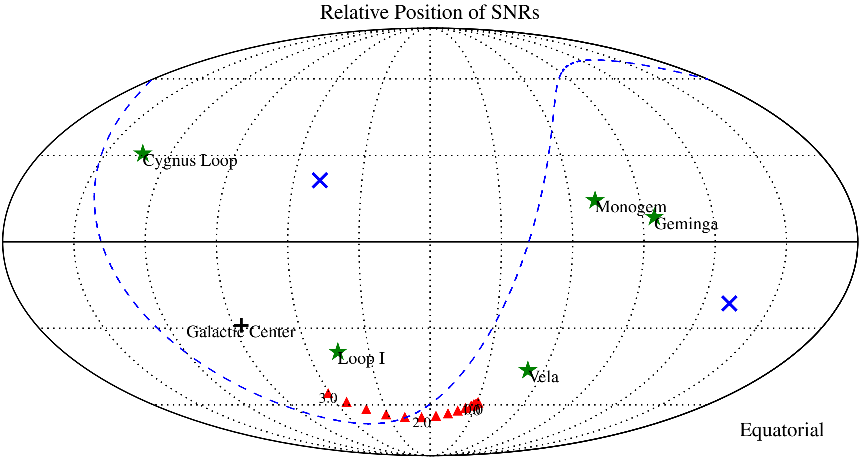

Relative position of the five closest known SNRs. The magnetic field direction (IBEX) is indicated by blue × and the **magnetic horizon** by a dashed line.

Phase-Flip by Vela SNR

- 1–100 TeV phase indicates dominance of a local source within longitudes:

$$120^\circ \lesssim l \lesssim 300^\circ$$

- **plausible scenario: Vela SNR** [MA'16]
  - *age* : $\simeq 11,000$ yrs
  - *distance* : $\simeq 1,000$ lyrs
  - *SNR rate* : $\mathcal{R}_{\rm SNR} = 1/30\,{\rm yr}^{-1}$
  - *(effective) isotropic diffusion*:

$$K_{\rm iso} \simeq 4\times 10^{28}(E/3{\rm GeV})^{1/3}{\rm cm}^2/{\rm s}$$

  - *Galactic half height* : $H \simeq 3$ kpc
  - *instantaneous CR emission* $(Q_\star)$

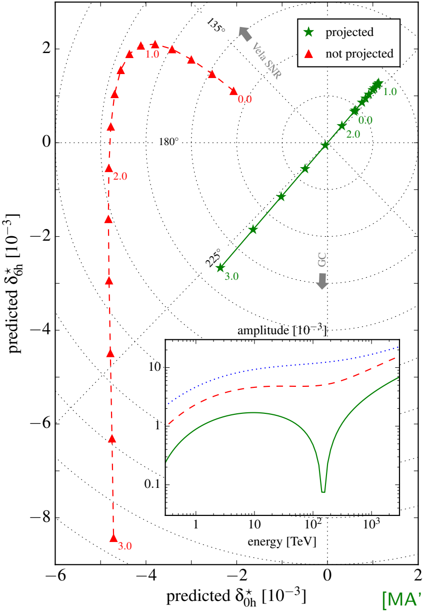

[MA'16]

Small-Scale Anisotropy

Small-Scale Anisotropy

- Significant TeV small-scale anisotropies down to angular scales of $\mathcal{O}(10)$ degrees.

- Strong local excess ("region A") observed by Northern observatories.

  [Tibet-ASγ'06; Milagro'08]
  [ARGO-YBJ'13; HAWC'14]

- Angular power spectra of IceCube and HAWC data show excess compared to isotropic arrival directions. [IceCube'11; HAWC'14]

$$C_\ell = \frac{1}{2\ell+1}\sum_{m=-\ell}^{\ell}|a_{\ell m}|^2$$

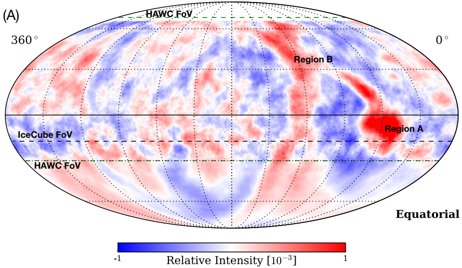

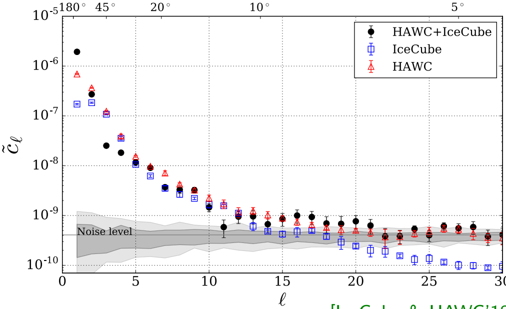

[IceCube & HAWC'18]

Small-Scale Anisotropy from Local Turbulence

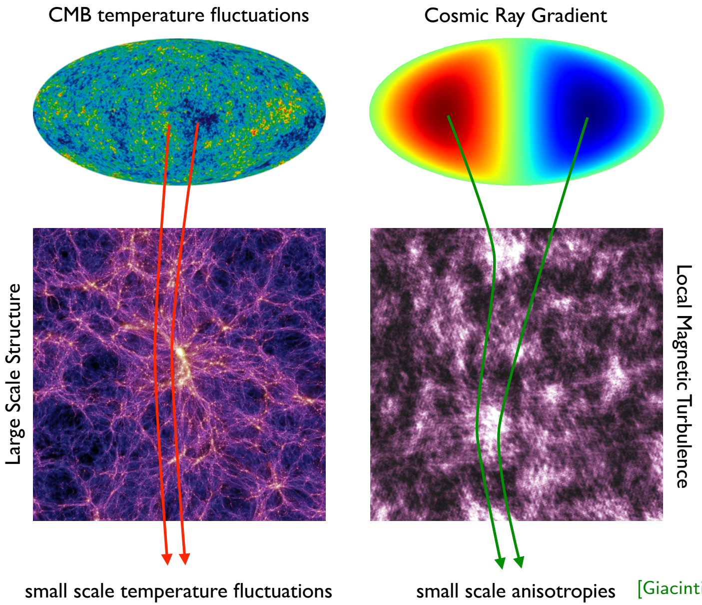

[Giacinti & Sigl'12]

Small-Scale "Theorem"

- *Assumptions:*
  - **absences of cosmic ray sources and sinks**
  - **isotropic and static** magnetic turbulence
  - initially, **homogeneous** phase space distribution

- *Theorem:* The sum over the ensemble-averaged angular power spectrum is constant:

$$\sum_{\ell}(2\ell+1)\langle C_{\ell}(t)\rangle = \text{const}$$

- Proof via **Liouville's theorem and angular auto-correlation function.** [MA'14]

➜ Wash-out of individual moments by diffusion (rate $\nu_\ell \propto \ell(\ell+1)$) has to be compensated by **generation of small-scale anisotropy**.

➜ Theorem implies small-scale angular features from large-scale average dipole anisotropy. [Giacinti & Sigl'12; MA'14; MA & Mertsch'15]

Comparison to CR Data

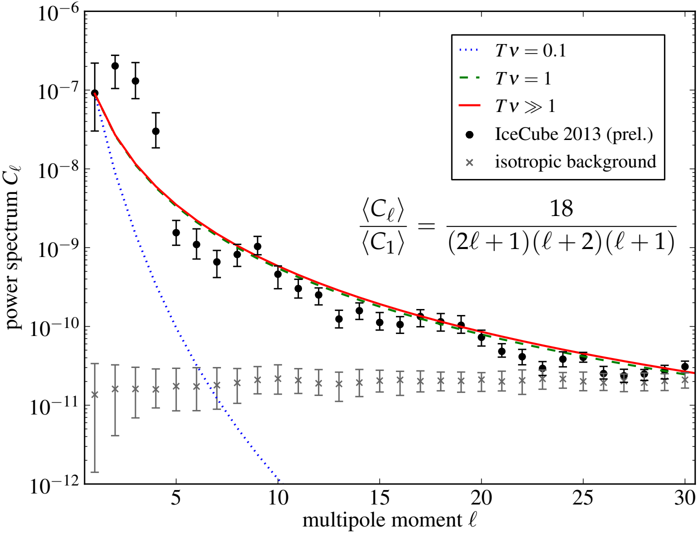

[MA'14]

Simulation via Backtracking

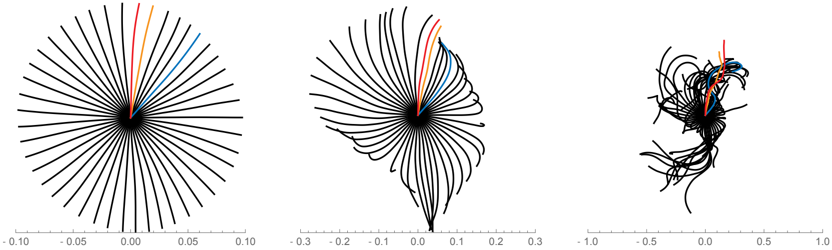

- Consider a local (quasi-)stationary solution of the **diffusion approximation**:

$$4\pi\langle f\rangle \simeq n_{\rm CR} + \underbrace{(\mathbf{r} - 3\,\widehat{\mathbf{p}}\,\mathbf{K})\nabla n_{\rm CR}}_{\text{1st order correction}}$$

- Ensemble-averaged C_ℓ's ($\ell \geq 1$): [MA & Mertsch'15]

$$\frac{\langle C_\ell\rangle}{4\pi} \simeq \int\frac{\mathrm{d}\hat{\mathbf{p}}_1}{4\pi}\int\frac{\mathrm{d}\hat{\mathbf{p}}_2}{4\pi}P_\ell(\hat{\mathbf{p}}_1\hat{\mathbf{p}}_2)\lim_{T\to\infty}\underbrace{\langle\mathbf{r}_{1i}(-T)\mathbf{r}_{2j}(-T)\rangle}_{\textit{relative}\text{ diffusion}}\frac{\partial_i n_{\rm CR}\partial_j n_{\rm CR}}{n^2_{\rm CR}}$$

Simulation via Backtracking

- simulation in isotropic & static magnetic turbulence with

$$\overline{\delta \mathbf{B}^2} = \mathbf{B}_0^2$$

- relative orientation of CR gradient:
  - solid lines : $\mathbf{B}_0 \parallel \nabla n$
  - dotted lines : $\mathbf{B}_0 \perp \nabla n$
- diffusive regime at $T\Omega \gtrsim 100$
- *enhanced* dipole predicions:

$$\langle C_1 \rangle > C_1 \text{ for } \langle f \rangle$$

- asymptotically **limited by simulation noise**:

$$\mathcal{N} \simeq \frac{4\pi}{N_{\rm pix}} 2TK^s_{ij} \frac{\partial_i n \partial_j n}{n^2}$$

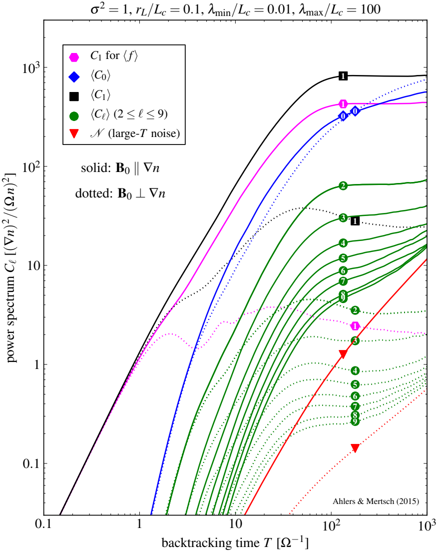

[MA & Mertsch'15]

Simulation vs. Data

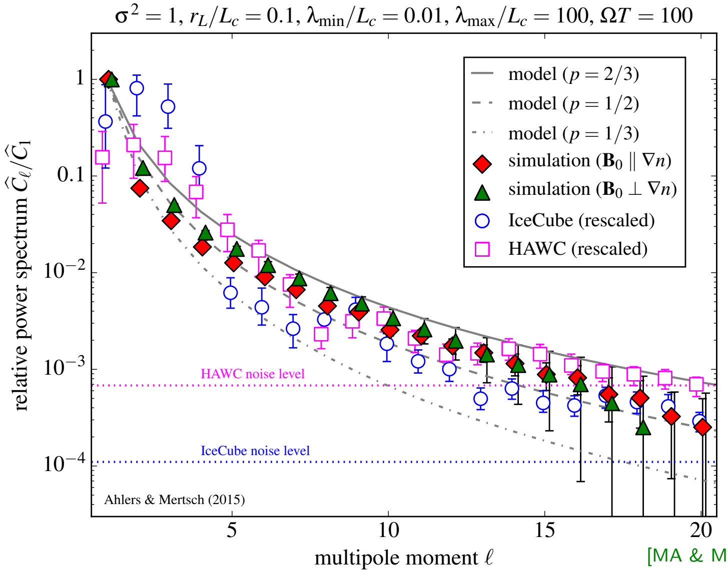

[MA & Mertsch'15]

Summary

- Observation of CR anisotropies at the level of **one-per-mille** is challenging.
- Reconstruction methods can **introduce bias**, sometimes not stated or corrected for.
- **Dipole anisotropy** can be understood in the context of standard diffusion theory:
  - TeV-PeV dipole phase aligns with local ordered magnetic field.
  - Amplitude variations as a result of local sources
  - Plausible & natural candidate: **the Vela supernova remnant**
- Observed CR data shows evidence of **small-scale anisotropy**.
  - Influenced by heliosphere?
  - Effect from non-uniform pitch-angle diffusion?
  - Result of local magnetic turbulence? ➜ **see also talk by G. Giacinti**

✔ Both observations allow to **probe our local Galactic environment.**

➜ **LHAASOs** prospective energy range (TeV–EeV), energy resolution and event statistics will allow to decipher large- and small-scale features in presently uncharted territory.

➜ Complements present and future Southern observatories (SWGO & IceCube-Gen2) for extended sky coverage in joint anisotropy analyses.

Appendix

KASCADE-Grande Data

- KASCADE-Grande in Karlsruhe, Germany (49.1° N, 8.4° E)
- data collected between March 2004 and October 2012
- available via: kcdc.ikp.kit.edu
- three energy bins from N_{ch} cuts:

data	E_{med}♣	N_{ch}-range	N_{tot}
sidereal solar	–	$\geq 10^{5.2}$	23,674,844
bin 1	2.7 PeV	$[10^{5.2}, 10^{5.6})$	17,443,774
bin 2	6.1 PeV	$[10^{5.6}, 10^{6.4})$	6,084,275
bin 3	33 PeV	$\geq 10^{6.4}$	146,795

- Full anisotropy construction in Northern Hemisphere possible with max-$\mathcal{L}$ method. [MA'19]

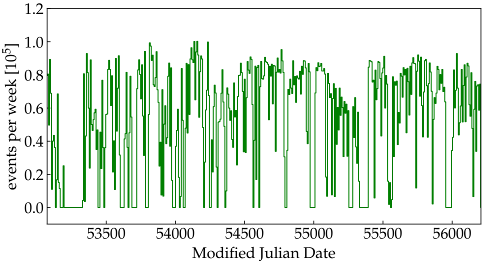

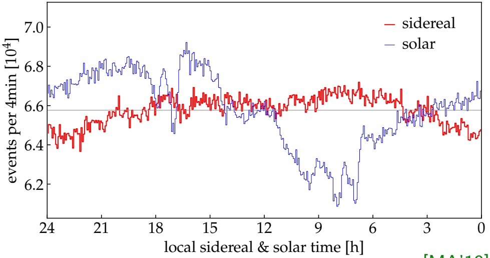

[MA'19]

Non-Uniform Pitch-Angle Diffusion

- stationary pitch-angle diffusion ($\mu \equiv \cos\theta$) :

$$v\mu \frac{\partial}{\partial z}\langle f \rangle = \frac{\partial}{\partial \mu} D_{\mu\mu} \frac{\partial}{\partial \mu}\langle f \rangle$$

- **non-uniform** diffusion:

$$\frac{D_{\mu\mu}}{1-\mu^2} \neq \text{const}$$

- non-uniform pitch-angle diffusion modifies the large-scale anisotropy aligned with $\mathbf{B}_0$
  - small scale excess/deficits for enhanced diffusion towards $\mu \simeq \pm 1$
    [Malkov, Diamond, Drury & Sagdeev'10]
  - modified large-scale features for enhanced diffusion at $\mu \simeq 0$ [Giacinti & Kirk'17]

➜ **talk by G. Giacinti**

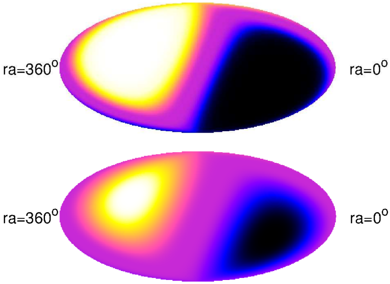

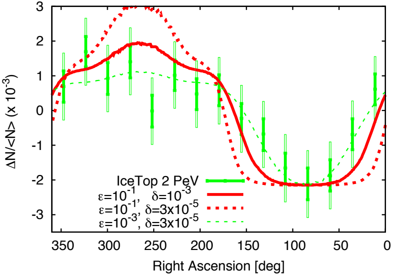

[Giacinti & Kirk'17]

Small-Scale Anisotropies from Heliosphere?

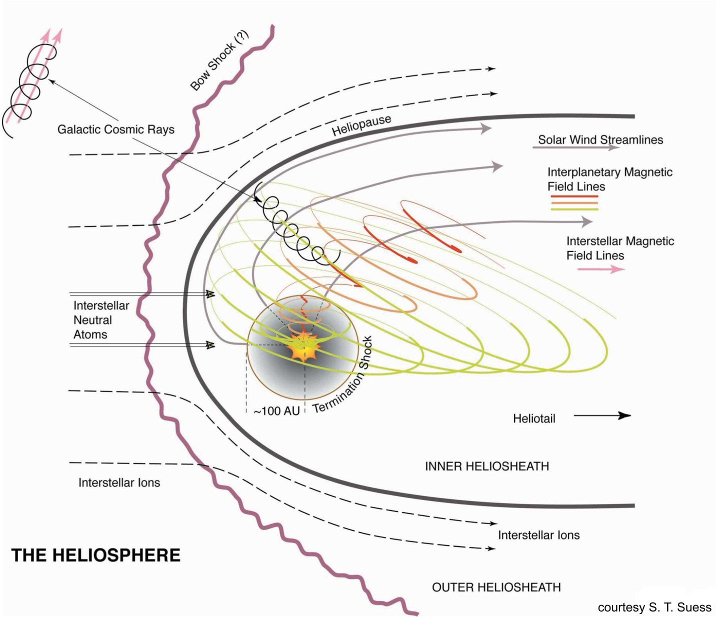

courtesy S. T. Suess

Small-Scale Anisotropies from Heliosphere?

- **Solar potential** affects cosmic ray flux (monopole) only at rigidity $\mathcal{R} \lesssim \mathrm{GV}$.
  [Gleeson & Axford'68;Gleeson & Urch'73]

- However, gyroradius of sub-TV cosmic rays smaller than the size of heliosphere:

$$r_g \simeq 200 \left(\frac{\mathcal{R}}{\mathrm{TV}}\right) \left(\frac{B}{\mu\mathrm{G}}\right)^{-1} \mathrm{AU}$$

- various effects and studies:
  - ⋆ hard CR spectra via magnetic reconnection in the heliotail [Lazarian & Desiati'10]
  - ⋆ non-isotropic particle transport in the heliosheath [Desiati & Lazarian'11]
  - ⋆ heliospheric electric fields induced by plasma motion [Drury'13]
  - ⋆ simulation via CR back-tracking in MHD simulation of heliosphere
    [Zhang, Zuo & Pogorelov'14; López-Barquero *et al.*'16]

Solar Potential

- dipole anisotropy induced by CR diffusion in solar wind:

$$|\mathbf{\Phi}| = -\underbrace{\frac{\beta_\odot(r)}{3}\frac{\partial\phi}{\partial\ln p}}_{\text{Compton-Getting}} \underbrace{-\kappa_\odot(r,p)\frac{\partial\phi}{\partial r}}_{\text{diffuse dipole}}$$

➜ **force-field approximation**: $|\mathbf{\Phi}| \simeq 0$ [Gleeson & Axford'68;Gleeson & Urch'73]

- local solution related to distribution beyond heliosphere:

$$\phi(r_\oplus, p(r_\oplus)) = \lim_{R\to\infty}\phi(R,p(R))$$

- $p(r)$ solution of **characteristic equation**:

$$\frac{\partial p}{\partial r} = \frac{\beta_\odot(r)}{3}\frac{p}{\kappa_r(r,p)}$$

➜ assume **Bohm diffusion** in heliosphere: $\kappa_\odot(r,p) \simeq \kappa_0(r)(\mathcal{R}/\mathcal{R}_0)$

$$p(r_\oplus) = p(\infty) - |Z|eV_\odot \qquad \text{with} \qquad V_\odot = \underbrace{\frac{\mathcal{R}_0}{3}\int_{r_\oplus}^{\infty}\mathrm{d}r'\frac{\beta_\odot(r')}{\kappa_0(r')}}_{\text{effective “solar potential”}} \lesssim 1\,\mathrm{GV}$$

Simulated Turbulence

- 3D-isotropic turbulence: [Giacalone & Jokipii'99]

$$\delta \mathbf{B}(\mathbf{x}) = \sum_{n=1}^{N} A(k_n)(\mathbf{a}_n \cos\alpha_n + \mathbf{b}_n \sin\alpha_n)\cos(\mathbf{k}_n \mathbf{x} + \beta_n)$$

- α_n and β_n are random phases in $[0, 2\pi)$, unit vectors $\mathbf{a}_n \propto \mathbf{k}_n \times \mathbf{e}_z$ and $\mathbf{b}_n \propto \mathbf{k}_n \times \mathbf{a}_n$
- with amplitude

$$A^2(k_n) = \frac{2\sigma^2 B_0^2 G(k_n)}{\sum_{n=1}^{N} G(k_n)} \qquad \text{with} \qquad G(k_n) = 4\pi k_n^2 \frac{k_n \Delta \ln k}{1 + (k_n L_c)^\gamma}$$

- Kolmogorov-type turbulence: $\gamma = 11/3$
- $N = 160$ wavevectors $\mathbf{k}_n$ with $|\mathbf{k}_n| = k_{\min} e^{(n-1)\Delta \ln k}$ and $\Delta \ln k = \ln(k_{\max}/k_{\min})/N$
- $\lambda_{\min} = 0.01 L_c$ and $\lambda_{\max} = 100 L_c$ [Fraschetti & Giacalone'12]
- rigidity: $r_L = 0.1 L_c$
- turbulence level: $\sigma^2 = \mathbf{B}_0^2 / \langle \delta \mathbf{B}^2 \rangle = 1$

Systematic Uncertainty of CR Dipole

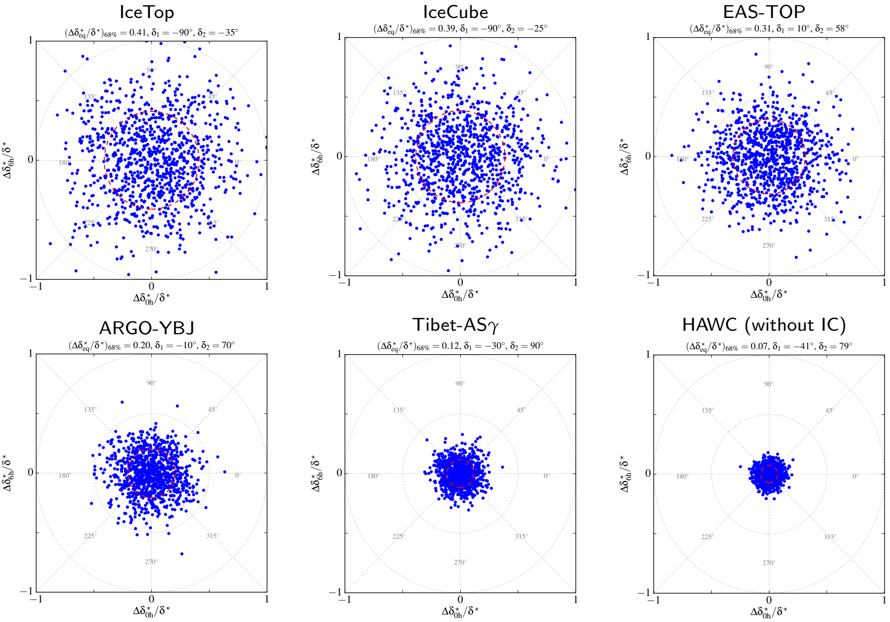

Compton-Getting Effect

- phase-space distribution is **Lorentz-invariant**

$$f(\mathbf{p}) = f^\star(\mathbf{p}^\star)$$

- **relative motion of observer** ($\boldsymbol{\beta} = \mathbf{v}/c$) in plasma rest frame ($\star$):

$$\mathbf{p}^\star = \mathbf{p} + p\boldsymbol{\beta} + \mathcal{O}(\beta^2)$$

- Taylor expansion:

$$f(\mathbf{p}) \simeq f^\star(\mathbf{p}) + (\mathbf{p}^\star - \mathbf{p})\nabla_{\mathbf{p}^\star} f^\star(\mathbf{p}) + \mathcal{O}(\beta^2) \simeq f^\star(\mathbf{p}) + p\boldsymbol{\beta}\nabla_{\mathbf{p}^\star} f^\star(\mathbf{p}) + \mathcal{O}(\beta^2)$$

➜ dipole term $\boldsymbol{\Phi}$ is **not invariant**:

$$\phi = \phi^\star \qquad \text{and} \qquad \boldsymbol{\Phi} = \boldsymbol{\Phi}^\star + \frac{1}{3}\boldsymbol{\beta}\frac{\partial \phi^\star}{\partial \ln p}$$

- with $\phi \sim p^{-2} n_{\rm CR} \propto p^{-2-\Gamma_{\rm CR}}$:

$$\boldsymbol{\delta} = \boldsymbol{\delta}^\star + \underbrace{(2+\Gamma_{\rm CR})\boldsymbol{\beta}}_{\text{Compton-Getting effect}}$$

✘ What is the plasma rest-frame? LSR or ISM : $v \simeq 20\text{km/s}$

Local Sources

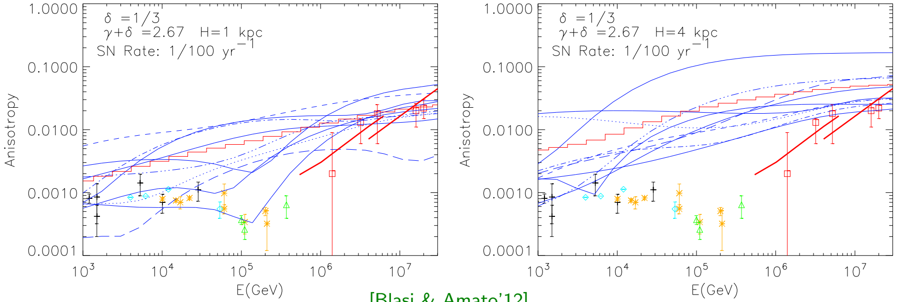

[Blasi & Amato'12]

- Distribution of local cosmic ray sources (SNR) in position and time induces variation in the anisotropy. [Erlykin & Wolfendale'06; Blasi & Amato'12] [Sveshnikova *et al.*'13; Pohl & Eichler'13]
- variance of amplitude can be estimated as: [Blasi & Amato'12]

$$\sigma_A \propto \frac{K(E)}{cH} \qquad \rightarrow \qquad \frac{\sigma_A}{A} = \text{const}$$

Local Magnetic Field

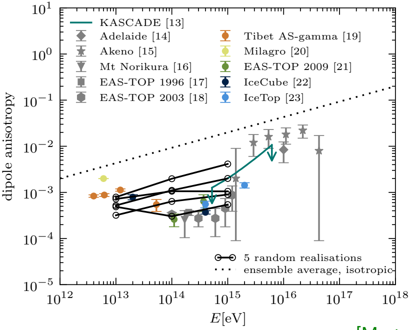

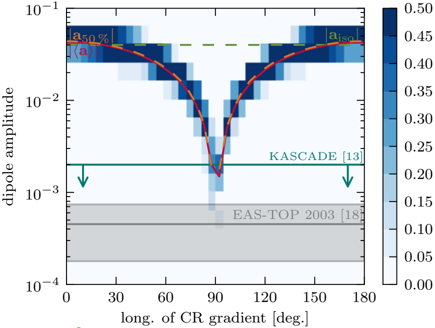

[Mertsch & Funk'14]

- **strong regular magnetic fields** in the local environment

➜ diffusion tensor reduces to **projector**: [*e.g.* Mertsch & Funk'14; Schwadron *et al.*'14; MA'17]

$$K_{ij} \to \kappa_{\parallel} \widehat{B}_i \widehat{B}_j$$

➜ **reduced** dipole amplitude and alignment with magnetic field: $\delta \parallel \mathbf{B}$

Local Magnetic Field

- **IBEX ribbon**: enhanced emission of energetic neutral atoms (ENAs) observed with Interstellar Boundary EXplorer [McComas *et al.*'09]
- interpreted as local magnetic field ($\lesssim 0.1$ pc) drapping the heliosphere
- circle center defines field orientation (in Galactic coordinate system): [Funsten *et al.*'13]

$$l \simeq 210.5^\circ \quad \& \quad b \simeq -57.1^\circ$$
$$(\Delta\theta \simeq 1.5^\circ)$$

- consistent with starlight polarization by interstellar dust ($\lesssim 40$ pc) [Frisch *et al.*'15]

$$l \simeq 216.2^\circ \quad \& \quad b \simeq -49.0^\circ$$

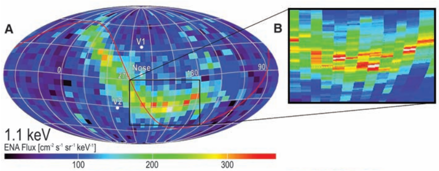

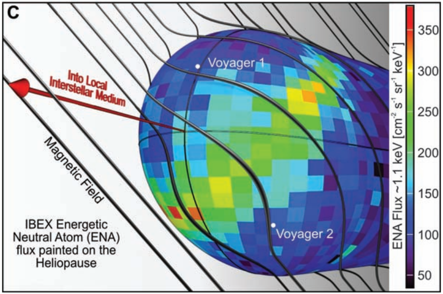

[McComas *et al.*'09]

Evolution Model

- Diffusion theory motivates that each $\langle C_\ell \rangle$ decays exponentially with an effective **relaxation rate** [Yosida'49]

$$\nu_\ell \propto \mathbf{L}^2 \propto \ell(\ell+1)$$

- A **linear** $\langle C_\ell \rangle$ evolution equation with generation rates $\nu_{\ell\to\ell'}$ requires:

$$\partial_t \langle C_\ell \rangle = -\nu_\ell \langle C_\ell \rangle + \sum_{\ell' \geq 0} \nu_{\ell' \to \ell} \frac{2\ell'+1}{2\ell+1} \langle C_{\ell'} \rangle \quad \text{with} \quad \nu_\ell = \sum_{\ell' \geq 0} \nu_{\ell \to \ell'}$$

- For $\nu_\ell \simeq \nu_{\ell\to\ell+1}$ and $\widetilde{C}_\ell = 0$ for $l \geq 2$ this has the analytic solution:

$$\langle C_\ell \rangle(T) \simeq \frac{3\widetilde{C}_1}{2\ell+1} \prod_{m=1}^{\ell-1} \nu_m \sum_n \prod_{p=1(\neq n)}^{\ell} \frac{e^{-T\nu_n}}{\nu_p - \nu_n}$$

- For $\nu_\ell \simeq \ell(\ell+1)\nu$ we arrive at a finite asymptotic ratio:

$$\lim_{T\to\infty} \frac{\langle C_\ell \rangle(T)}{\langle C_1 \rangle(T)} \simeq \frac{18}{(2\ell+1)(\ell+2)(\ell+1)}$$

Another Example: Pierre Auger

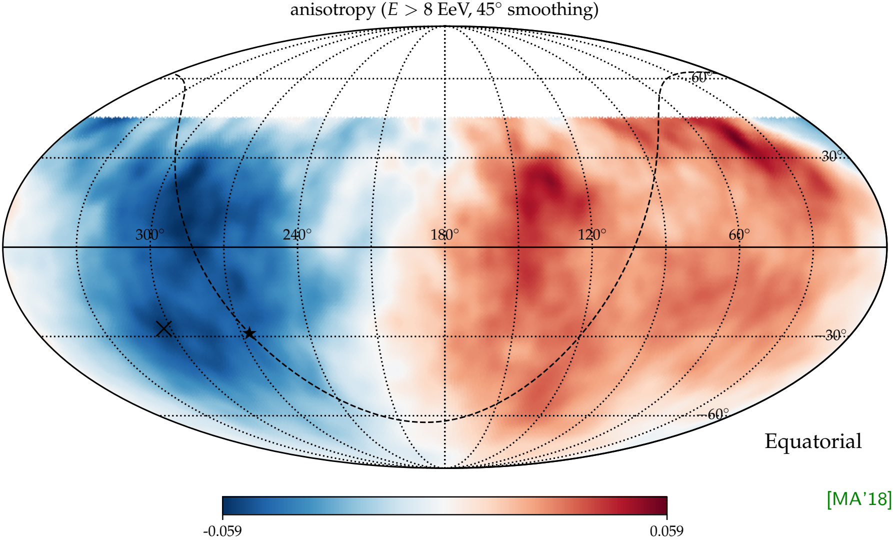

[MA'18]

Method can also be applied to high-energy data beyond the knee, *e.g.* Auger.

Another Example: Pierre Auger

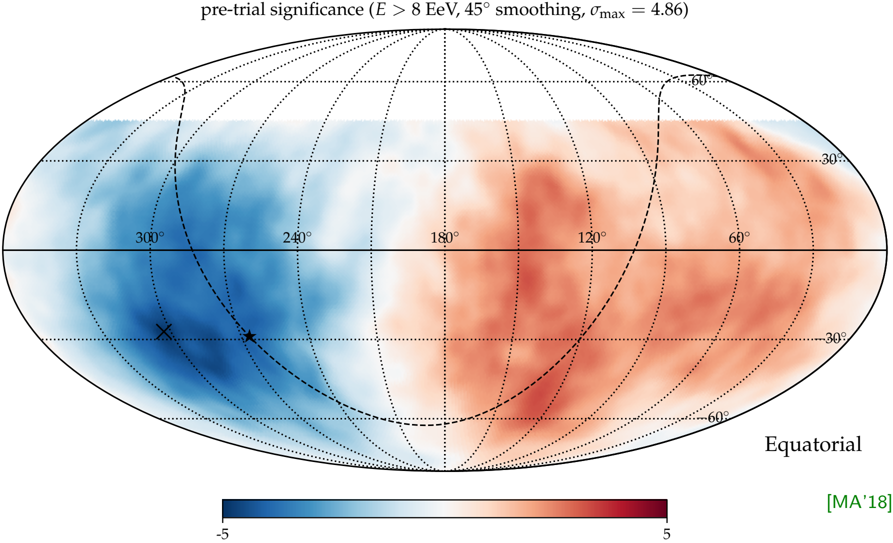

[MA'18]

Method can also be applied to high-energy data beyond the knee, *e.g.* Auger.